Conformational Studies of Vibrational Properties and Electronic States of Leucoemeraldine Base and Its Oligomers

ARTICLE *in* MACROMOLECULES · FEBRUARY 1997

Impact Factor: 5.8 · DOI: 10.1021/ma961120n

2 AUTHORS:

Cheol Ho Choi
Kyungpook National University
111 PUBLICATIONS **2,123** CITATIONS
SEE PROFILE

Miklos Kertesz
Georgetown University
226 PUBLICATIONS **6,597** CITATIONS
SEE PROFILE

Conformational Studies of Vibrational Properties and Electronic States of Leucoemeraldine Base and Its Oligomers

Cheol Ho Choi and Miklos Kertesz*

Department of Chemistry, Georgetown University, Washington, DC 20057-1227

Received July 26, 1996; Revised Manuscript Received November 5, 1996[⊗]

ABSTRACT: *Ab initio* geometry optimizations and normal mode analysis have been performed on a series of oligomers of leucoemeraldine base (LB, the fully reduced amine form of polyaniline) over conformational variations with the HF/6-31G* basis set. Aniline was used to obtain 12 force constant scaling factors with the best vibrational frequency root mean square error of 5.2 cm^{-1}. These scaling factors are used in the analysis of the vibrational spectra of diphenylamine, *N*,*N*′-diphenyl-1,4-phenylenediamine, aniline end-capped trimer, and LB. A polymeric normal mode analysis has been performed using the scaled quantum mechanical oligomer force field (SQMOFF) method where polymer force fields are constructed from the extrapolation of scaled *ab initio* oligomer force fields. CN stretching, NH rocking, and CH in-plane bending modes are strongly affected by the molecular conformation. The peaks around 1220 and 1180 cm^{-1} in the Raman spectrum turn out to be indicators of molecular and polymeric planarity. The differences between Raman spectra of Quillard *et al.* and Furukawa *et al.* of *N*,*N*′-diphenyl-1,4-phenylenediamine can also be explained by differences of the molecular conformation of the different samples. The energetics of isolated chains favors a nonplanar conformation by about 3−4 kcal/mol per phenyl ring, but intermolecular interactions seem to influence the favored conformations of various oligomers. On the basis of IR and Raman spectroscopic evidence, most probable conformations for each oligomer and the LB polymer are proposed. A complete assignment of LB vibrational frequencies including symmetries of each normal mode has been achieved with excellent agreement with the published experimental values. We have found that, as the size of the oligomer is increased, planarity increases. This preference of planarity in leucoemeraldine base was further supported by our band calculation using MEHT (modified extended Hückel theory).

1. Introduction

Vibrational spectroscopy has the potential to yield valuable structural and conformational information on polymers, if used in conjunction with accurate quantum mechanical vibrational calculations. In this paper we attempt to resolve structural questions for an important member of the polyaniline family of polymers.

Polyaniline has been studied extensively in the last few years for its high conductivity.[1] Owing to the nitrogens which are incorporated between the phenyl rings of the backbone, polyaniline can have a variety of forms conformationally and structurally. The structure of polyaniline can be distinguished by the oxidation state[2] of the nitrogen atom as leucoemeraldine base (LB, 100% amine form), emeraldine base (EB, 50% amine form), and pernigraniline base (PNB, 100% imine form); the fully reduced, half-oxidized, and fully oxidized forms of polyaniline, respectively (see Figure 1). Furthermore, for any given oxidation state a large degree of conformational variation exists concerning the torsional orientation of the phenyl rings. This variation arises from the competition of the p−π conjugation of the bridging nitrogens and the steric hindrances arising from adjacent hydrogens.

Generally, conjugated polymers exhibit strong coupling between the electronic structure and certain geometric degrees of freedom.[1d−f,3] In this context, the role of conformational effects, specifically phenyl ring torsional angles, on the electronic and vibrational properties is one of the fundamental issues in these kinds of conducting polymers. There have been several theoretical studies[1d−f,4,5] showing the importance of ring torsional conformation in determining the ground-state electronic structure and geometry of the polyaniline. Brédas *et al.*[1d] have shown that in the case of the LB form, which in the ground state has no Peierls contribution to the gap, the influence of ring-torsion dimerization is negligible and the electronic band gaps primarily arise from the HOMO and LUMO of the phenyl rings. On the contrary, in the case of PNB, which in the ground state possesses a Peierls gap, ring torsion contributes to as much as about 40% of the full band-gap value, while the rest can be traced back to the symmetry breaking of the bond distance pattern related to the presence of two kinds of rings (aromatic and quinonoid) in this form of polyaniline. The charge carriers such as soliton, polaron, and bipolaron defect states in polyaniline have been proposed to arise partly from changes in local ring-torsional conformation.[4,5]

Starikova[6] has analyzed the experimentally determined structures of dozens of amino compounds and has pointed out that the phenyl ring torsional angles, the pyramidality (the sum of the bond angles around nitrogen), and the deviations of the nitrogen(s) from the planes of the attached phenyl ring should be all analyzed together. Because of its inherent difficulties, however, there are no detailed geometrical data available for polyaniline from experiment, including LB. There have been several semiempirical and *ab initio* studies[1d−f,7] on amino aryl systems and oligomer models for polyaniline. For instance, Brédas *et al.*[1d] has concluded that the bridging nitrogen in LB has sp^2 character based upon bond lengths and angles resulting from semiempirical AM1 calculations. (They used these geometrical data as input for energy band calculations.) AM1 geometry calculations, however, could not correctly reproduce the two nonidentical torsional angles of diphenylamine. Higher level calculations on these systems are expected to provide quantitatively more accurate results.

[⊗] Abstract published in *Advance ACS Abstracts,* February 1, 1997.

S0024-9297(96)01120-5 CCC: $14.00

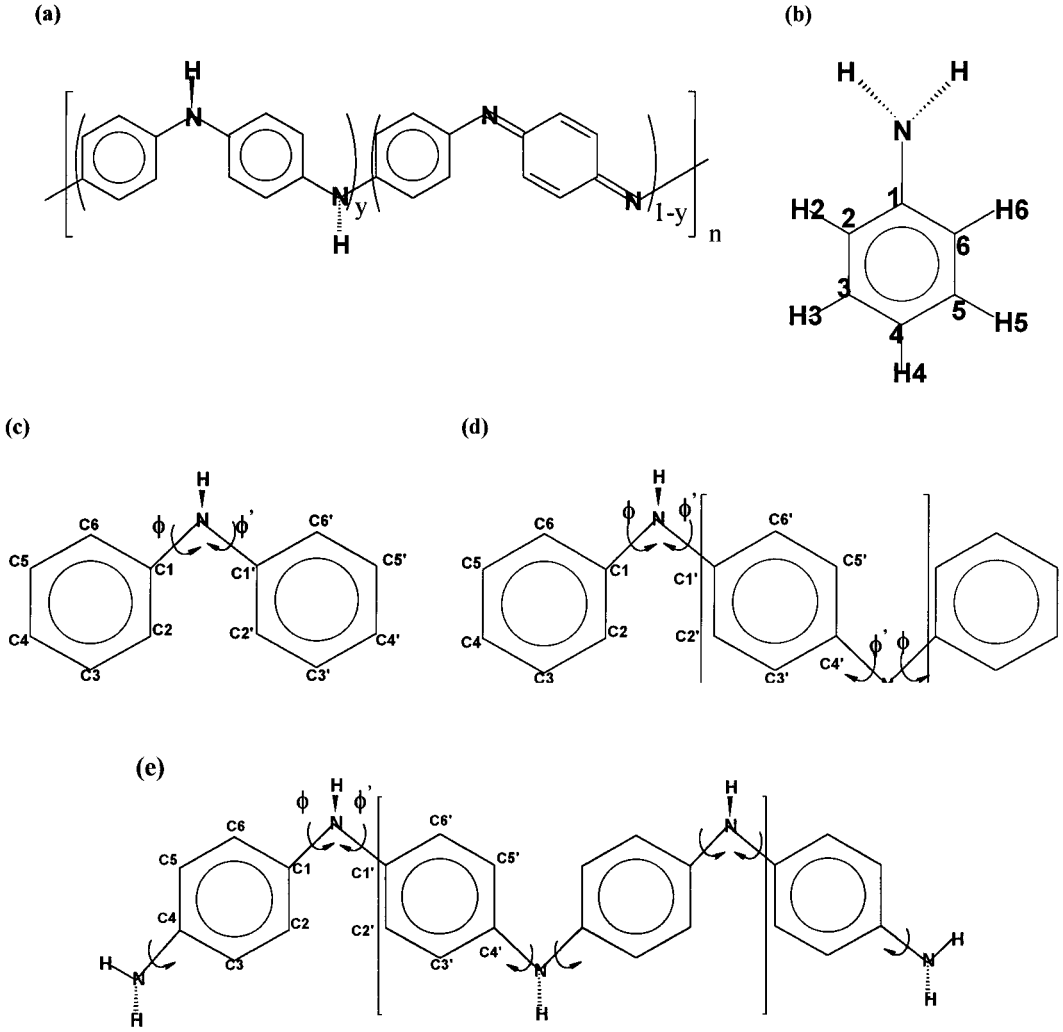

Figure 1. (a) Leucoemeraldine base (LB), emeraldine base (EB), and pernigraniline base (PNB) refer to the different oxidation states of the polymer where $y = 1$, 0.5, and 0, respectively. (b) Aniline. (c) Diphenylamine. (d) *N*,*N*′-Diphenyl-1,4-phenylenediamine or phenyl end-capped dimer (PCD). (e) Aniline end-capped trimer (ACT). The unit cells for polymeric normal mode analysis and energy band calculations are indicated by square brackets in structures d and e.

Since electronic properties of conjugated systems are strongly coupled with the backbone geometry of the polymer, a great number of studies have been devoted to the study of their vibrational properties, both experimentally and theoretically.[8] Recently, Quillard *et al.*[8b,c] have analyzed the vibrational spectra of polyaniline assuming a planar structure and focused on in-plane vibrational modes. They assumed that the vibrational modes resulting from ring stretching and N−H bending in the 1500 cm^{-1} region may be affected only slightly, an assumption that could be justified if the in-plane modes would not strongly couple with phenyl ring torsional angles. However, since π conjugation of this polymer is related to the phenyl ring torsional angle, the backbone of polyaniline may be affected by the torsional angles. Aspects of conformational effects on the vibrational properties of polyanilines have not been studied yet.

The object of this study is to understand the relationships between conformations and vibrational properties of LB and its oligomers, so as to propose a most probable conformation for LB. We have chosen aniline, diphenylamine (DPA), *N*,*N*′-diphenyl-1,4-phenylenediamine (or phenyl end-capped dimer, PCD), and aniline end-capped trimer (ACT) as model compounds (see Figure 1). Based on the normal mode study of these oligomers and the LB polymer, a complete assignment of the vibrational frequencies of LB is also attempted. Combining the geometrical and vibrational data, the evolution of conformation of this polyaniline is discussed. In addition, energy band calculation based on *ab initio* geometric parameters are performed to study conformation-dependent energy band structures.

2. Computational Method

The scaled quantum mechanical oligomer force field (SQMOFF)[9] method has been successfully applied for the interpretation of the vibrational spectra of several polymeric systems[10] and was used for the polymeric vibrational analysis in this study. The basic idea behind this method is that, if we assume an ideal polymer which has a translational (or helical) symmetry, one can apply the Born−Karman cyclic boundary conditions[11] and thereby reduce the vibrational problem from one of infinite dimensions to NKP number of finite $P \times P$ diagonalizations, where NKP is the representative number of *k*-points in the Brillouin zone (e.g., 13) and *P* is the number of vibrational degrees of freedom of each translational unit.

Consequently, the force field matrix of the ideal polymer which now has *k*-dependency can be described by

$$F_k = F_0 + \sum_{q=-m}^{m} F(q)e^{ikaq} \qquad (1)$$

where F_0 is a central unit's force constant matrix, $F(q)$ is a

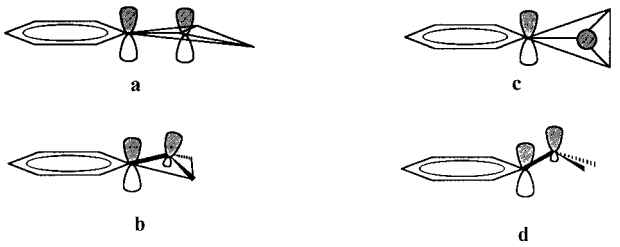

Figure 2. Possible conformations of aniline suggested by Starikova (after ref 6).

qth coupling force constant matrix, m is the number of interacting neighboring unit cells, and kaq represents the phase difference between the neighboring cells at any given k. The $F(q)$ blocks of the force field can be extrapolated from the complete force matrix of appropriately chosen oligomers. Because of fast convergence of coupling force constants, we only need the center block ($q = 0$) and first interacting block ($q = 1$) to correctly describe the k-dependent polymer force field.[9] Eigenvalues and eigenvectors of polymer normal modes are given in Cartesian coordinates by

$$GF(k)\, L_i(k) = \lambda_i L_i(k) \qquad (2)$$

where G is Wilson's G matrix[12] of the unit cell, $L_i(k)$ is the k-dependent eigenvector of the ith normal mode, and λ_i is corresponding eigenvalue proportional to the square of the frequency and is a function of k.

The equilibrium geometry, the unscaled force constants, and the derivatives of the dipole moment and polarizability of the oligomers have been calculated at the *ab initio* Hartree−Fock level by the Gaussian 94[13] package and a 6-31G* basis set. (We have found that in order to get a good conformational description, specifically ring torsional angles of polyaniline, at least a 6-31G* basis set is required.) Because of the level of theory of the *ab initio* method, the calculated vibrational frequencies are always overestimated.[14] Pulay's modified scaling scheme[15] was utilized to scale the calculated frequencies.

First, we attempted to perform a nonuniform scaling of the force constants according to Pulay's original scheme.[16] Unfortunately, this did not yield a satisfactorily small root mean square error of the fit for the aniline molecule. We have identified three groups of off-diagonal force constants for aniline and assigned each group its own scaling factor. The selected three off-diagonal groups are the following: C−C stretching/C−C stretching, C−H in-plane bending/ring torsion, and C−C or C−N stretching/ring deformation coupling. Using an additional off-diagonal scaling factor for each of these groups, we have obtained a rather small (5.2 cm^{-1}) overall root mean square error as compared with the experimental frequencies.[17]

Modified extended Hückel band calculations (MEHT)[18] have been performed using *ab initio* optimized geometries. The optimized geometric data of the center block of planar PCD and ACT have been used as planar and nonplanar structures of the polymer, respectively.

All simulated spectra were produced by a Lorentzian broadening with fwhm of 3.0 cm^{-1}. Calculated spectra are presented with peak heights proportional to the absolute intensities within in each figure, but not across different figures. IR and Raman intensities were calculated from the dipole moment derivatives and polarizability derivatives of the oligomers, as described in ref 9.

3. Aniline: Structure and Vibrational Spectra

Starikova[6] has proposed four different configurations of substituted anilines (see Figure 2) according to the hybridization of nitrogen and suggested model b as the most realistic model, in which the plane of the surrounding atoms is not the same as the phenyl ring plane. The maximum conjugation occurs between the phenyl ring and the nitrogen in model a, whereas models d and c have small and no conjugation, respectively.

Table 1. Geometric Parameters of Aniline

	exptl[a]	HF/6-31G* [b]	calcd[a]
C1−C2	1.397	1.393	1.401
C2−C3	1.394	1.383	1.392
C3−C4	1.396	1.386	1.395
C1−N	1.402	1.397	1.415
N−H	1.001	0.997	1.007
C2−H2	1.082	1.077	1.080
C3−H3	1.083	1.076	1.079
C4−H4	1.080	1.075	1.078
C6−C1−C2	119.4	118.7	118.7
C1−C2−C3	120.1	120.4	120.5
C2−C3−C4	120.7	120.9	120.7
C3−C4−C5	118.9	118.8	119.0
N−C1−C2	120.3	120.6	120.6
H2−C2−C3	120.1	120.0	120.1
H3−C3−C4	120.0	120.0	120.0
H4−C4−C3	120.5	120.6	120.5
H−N−C1		114.3	111.2
H−N−H	113.1	110.7	108.1
δ[c]	37.5	41.0	55.6

[a] Reference 22. [b] This work. [c] Angle between C−N bond and NH_2 plane.

Table 2. Optimized Scaling Factors Obtained for Aniline

group coordinates[a]	scaling factors
C−C stretching	0.8684
C−N stretching	0.9100
C−H stretching	0.8285
N−H stretching	0.8126
torsion, NH_2 scissoring, NH_2 rocking, and NH_2 wagging	0.7703
trigonal def, antisym def, and antisym def.′	0.7790
puckering, antisym torsion, and antisym torsion′	0.8079
in−plane bending (C−N)	0.9202
in−plane bending (C−H)and out−of−plane bending (C−N and C−H)	0.7935
C−C/C−C coupling	0.6719
out−of−plane bending/ring torsion	1.2709
C−C, C−N stretching/ring deformation	0.9830

[a] Group coordinates are defined in ref 15.

The hybridization of nitrogen of Starikova's model b is between sp^2 and sp^3 character. The experimental and also our calculated angles of H−N−C1 and H−N−H are close to 109°, indicating sp^3 character of the nitrogen atom (see Table 1). Furthermore, the angle δ deviates from the phenyl plane ring significantly. Since the nitrogen is almost in the same plane as the phenyl ring, however, there still exists significant $p-\pi$ conjugation between the nitrogen and the phenyl ring. Therefore, the nitrogen can be described as mostly sp^2 with some partial sp^3. Because of quite good overall agreement with the experimental geometry, HF/6-31G* theory seems to be proper for this study, especially, because the scaled calculated vibrational frequencies are also excellent.

As we mentioned earlier, nine diagonal scaling factors were augmented with three off-diagonal ones in determining the best scaling factors by error minimization. The final scaling factors are presented in Table 2 with a 5.2 cm^{-1} root mean square error. It should be noted that the out-of-plane bending/ring-torsion coupling scaling factor is larger than 1. The calculated and the experimental frequencies are presented in Table 3. We think that these three off-diagonal factors are critical for reasonable scaling. The NH_2 wagging mode around 658−669 cm^{-1} was not included in the scaling procedure because of its strong dependency on the different

Table 3. Observed and Calculated Frequencies of Aniline[a] (in cm^{-1})

exptl[b]	scaled HF/6-31G*	assignments
3500	3503	NH_2 stretch
3418	3415	NH_2 stretch
3088	3083	CH stretch
3072	3067	CH stretch
3053	3055	CH stretch
3037	3038	CH stretch
3025	3032	CH stretch
1618	1620	NH_2 scissoring
1603	1594	ring stretch
1590	1592	ring stretch
1503	1502	ring stretch
1468	1474	ring stretch
1330	1335	CH in-plane bend
1308	1309	CC stretch + CN in-plane bend
1278	1276	CN stretch
1173	1178	CH in-plane bend
1152	1150	CH in-plane bend
1115	1115	NH_2 rocking + CH in-plane bend
1054	1047	NH_2 Rocking
1028	1033	CH in-plane bend
996	986	ring breathing
968	967	CH out-in-plane bend
957	962	trigonal def
874	882	CH out-of-plane bend
823	826	CH out-of-plane bend
808	813	CC stretch + ring def
747	756	CH out-of-plane bend
689	693	puckering
(670)[c]	636	NH_2 wagging
619	614	antisym def′
526	524	antisym. def
500	496	antisym. torsion
415	411	antisym torsion′
390	389	CN in-plane bend
233	221	antisym torsion
216	220	NH_2 torsion

[a] The overall root mean square error is 5.2 cm^{-1}. [b] Taken from ref 17. [c] The frequency in parentheses is not included in the scaling process. (See text.)

experimental environments.[17a] In solution this band is at 570 cm^{-1}, and the liquid phase data are 650−670 cm^{-1}. In any case, this mode is not present in the polymer.

Most of the original assignments[17a] are in agreement with our accurate *ab initio* results, with the exception of the following modes: the 1130, 1115, 957, and 808 cm^{-1} bands are reassigned as C−H in-plane bending, NH_2 rocking + C−H in-plane bending, ring trigonal deformation, and ring deformation modes, respectively.

All scaling factors (see Table 2) were transferred to be used in the vibrational analysis of the other oligomers. A nontrivial aspect of this transfer of scaling factors is that the scaling factors of scissoring, rocking, and wagging modes of the amino group in aniline were transferred to the scaling factors of the C1−N−C1′ bending, NH rocking, and NH wagging modes of the imino group in the other oligomers, respectively. This approximation might affect the corresponding scaled frequencies especially in the low-frequency region. Fortunately, the normal modes of the NH rocking mode are very well reproduced in DPA, confirming the validity of this intuitive transfer of scaling factors.

4. Geometries of Oligomers

First we discuss briefly the geometries of each of the oligomers discussed in the paper, with emphasis on the conformational flexibility around the phenyl torsions. This discussion will be followed by the vibrational analysis of the oligomers and the LB polymer. When the energy difference between the two conformers is too small to determine which one is preferred, we use vibrational spectroscopy data and the respective theoretical fits to decide the actual conformation.

A. DPA. The bridging nitrogen in DPA is connected to two phenyl rings, and the effect of steric repulsion arises from the proximity of the phenyl rings and thereby plays an important role in influencing its conformation, which can be represented by two torsional angles, ϕ (C2−C1−N−C1′) and ϕ' (C1−N−C1′−C2′) (see Figure 1). Ito *et al.*[7] have proposed four possible conformations of DPA using these two angles. However, their "book" and "Morino" forms are high in energy. Their skewed form requires that $\phi = -\phi'$, which is what they obtained in their STO-3G geometry optimization. However, this is not in agreement with experiment: the amine H is not in the C1−N−C1′ plane.[6]

It is more realistic to consider three conformations (C_1, C_s, and C_{2v}) using two torsional angles. In C_1, the two independent torsional angles have different magnitudes with opposite sign. In C_s, the two torsional angles are identical and have the same sign. The C_{2v} conformation is planar. These conformations are influenced by conjugation and steric repulsion. Fully optimized geometric data of our proposed conformations are presented in Table 4. Energetically, the C_1 conformation is the most stable by about 3−4 kcal/mol as obtained by the HF/6-31G* calculations. The calculated C−N bond lengths vary over the 1.393−1.423Å range, which correspond to typical bond lengths of aromatic substituted C−N bonds.[6] Due to the strong repulsion, the C1−N−C1′ angle is increased to the rather large value of 135.8° in the C_{2v} conformation. It can be seen that our geometrical parameters in the C_1 conformation reproduce the experiment very well, including the bond lengths and the C1−N−C1′ angle, and clearly show two different ring-torsional angles, 13.9° and 48.8°. According to the HF/STO-3G[7] and the semiempirical calculations,[1d] however, the most stable conformation of DPA has been suggested to have identical ring-torsional angles with opposite sign ($\phi = -\phi'$). This difference turns out to be crucial in the description of the vibrational spectra in the next section.

The out-of-plane angle of the hydrogen atom attached to nitrogen with respect to the C1−N−C1′ plane can also be a good indicator of the degree of hybridization of the nitrogen atom. In the C_1 conformation, this angle (26.3°) actually breaks the $\phi = -\phi'$ symmetry and, consequently, leads to two different torsional angles. It has turned out that the vibrational intensities of the modes attributed to NH rocking are strongly affected by these angles (see sections 5 and 6). HF/6-31G* theory seems to correctly describe the balance of p−π conjugation and H−H steric repulsion in DPA, at least qualitatively.

B. PCD. PCD is an interesting molecule in that it is the smallest oligomer incorporating a disubstituted benzene and can therefore be considered intermediate between DPA and polyaniline. Possible molecular conformations of PCD might correspond to the C_i or C_{2h} point group. Geometry optimization and normal mode analysis within these two point groups have been performed. Similar to DPA, the two ring-torsional angles, C2−C1−N−C1′ (ϕ) and C1−N−C1′−C2′ (ϕ'), were used to distinguish the two conformations (see Figure 1). The C_{2h} conformation is defined by $\phi = \phi' =$

Table 4. Optimized Geometrical Parameters and Relative Energies of Diphenylamine (DPA)[a]

	this work						
	C_s	C_1	C_{2v}	exptl[d]	exptl[e]	calcd[f]	calcd[g]
N−C1	1.423	1.402	1.393	1.401	1.40	1.424	1.396
N−C1′	1.423	1.401	1.393	1.406	1.40	1.424	1.396
C1−C2	1.390	1.391	1.392				
C1′−C2′	1.390	1.394	1.392				
C2−C3	1.384	1.386	1.389				
C2′−C3′	1.384	1.383	1.389				
C3−C4	1.386	1.383	1.380				
C3′−C4′	1.386	1.387	1.380				
C4−C5	1.384	1.387	1.388				
C4′−C5′	1.384	1.384	1.388				
C5−C6	1.385	1.381	1.377				
C5′−C6′	1.385	1.385	1.377				
C6−C1	1.390	1.395	1.402				
C6′−C1′	1.390	1.391	1.402				
C1−N−C1′	119.7	126.6	135.8	124.5	126	128.4	125.9
N−C1−C2	121.1	123.4	126.7				
N−C1′−C2′	121.1	121.3	126.7				
C1′−N−C1−C2 (ϕ)	74.3	13.9	0	23.0		26.2	27.7
C1−N−C1′−C2′ (ϕ')	74.3	48.8	0	36.9		26.2	27.7
H out-of-plane[b]	51.2	26.3	0	24.4		0	0
relative energy[c]	3.36	0	4.12				

[a] Atom numbering is defined in Figure 1. [b] Angle with respect to C1−N−C1′ plane. [c] In kcal/mol. [d] From ref 6. [e] From ref 7. [f] From ref 23, with STO-3G basis set. [g] From ref 1d, with AM1.

Table 5. Optimized Geometrical Parameters and Relative Energies of PCD and ACT[a]

	PCD			
	this work			ACT
	C_i	C_{2h}	exptl[d]	this work
N−C1	1.401	1.389	1.399	1.424
N−C1′	1.411	1.398	1.416	1.430
C1−C2	1.391	1.393		1.394
C1′−C2′	1.389	1.391		1.389
C2−C3	1.387	1.389		1.383
C2′−C3′	1.384	1.382		1.386
C3−C4	1.383	1.379		1.391
C3′−C4′	1.389	1.393		1.393
C4−C5	1.387	1.389		1.389
C4′−C5′	1.389	1.391		1.386
C5−C6	1.380	1.377		1.386
C5′−C6′	1.384	1.382		1.385
C6−C1	1.396	1.403		1.385
C6′−C1′	1.389	1.393		1.388
C1−N−C1′	124.6	135.5	128.9	121.0
N−C1−C2	123.4	126.6		121.8
N−C1′−C2′	120.5	127.3		120.5
C1′−N−C1−C2 (ϕ)	0.10	0	20.0	15.5
C1−N−C1′−C2′ (ϕ')	66.6	0	16.0	87.5
H out-of-plane[b]	29.5	0		
rel energy[c]	0	9.2		

[a] Atom numbering is defined in Figure 1. [b] The angle with respect to the C1−N−C1′ plane. [c] In kcal/mol. [d] From ref 6.

0, while in the C_i conformation, they are optimized independently.

As expected, the C_i form is more stable by 9.2 kcal/mol at the HF/6-31G* level of theory. At this level all geometric parameters are quite well reproduced except the two ring-torsional angles (see Table 5). The calculated results ($\phi = 0.1°$ and $\phi' = 66.6°$ in C_i) correspond to good p−π conjugation between the two end phenyl rings and the two nitrogen atoms and almost no p−π conjugation between the middle phenyl ring and the two nitrogen atoms. Consequently, the N−C1′ bond length is somewhat longer than N−C1. These torsional-angle discrepancies might arise from the level of theory. Also, the relatively soft potential surface along ϕ and ϕ' may be strongly influenced by intermolecular interactions. Due to these ring-torsional discrepancies, the normal mode analysis using these geometric data will only be the starting point in the process leading to the understanding of conformational effects on the vibrational spectra of polyanilines.

C. ACT. ACT is the next oligomer in the sequence. It serves as a model for the geometry and force field of nonplanar LB. Its geometry is described in Table 5. No experimental data are available for the geometry of ACT, but its similarity to PCD (C_i) is obvious. Because of lack of inversion symmetry in ACT, a full geometry optimization will give a bent form. Therefore, we have restricted all nitrogen atoms to be in the same plane. The geometry optimization of ACT and the subsequent normal mode analysis were performed under this constraint, which allows the extrapolation to an infinite periodic LB polymer.

In this study we have adopted the following approach: we vary ϕ and ϕ' in such a way as to obtain the best agreement between the calculated and experimental vibrational spectra, without introducing any other parameters in addition to the aniline scaling factors discussed earlier. Then we use the spectral predictions to obtain indirect information on the conformation.

5. Raman Spectra of Leucoemeraldine Base and Its Oligomers

Since molecular planarity is related to conjugation, some vibrational frequencies and intensities are significantly affected by molecular conformation. Theoretical simulations of the vibrational spectrum with several possible conformations, therefore, might shed light on the structure through understanding of the conformational dependence of the vibrational spectra. The predicted and experimental Raman and IR spectra have been collected in Table 6a,b. This also allows the comparative assignment of the oligomer and polymer modes. For the oligomers only those modes are given that carry significant intensity or correspond to peaks with nonzero intensity in the LB polymer.

A. DPA. The calculated force constants of DPA were scaled by the scaling factors determined for aniline as described in section 3. The C−C stretching region around 1605 and 1588 cm^{-1} in the Raman spectrum (see Figure 3a and Table 6a) is less sensitive to the variation

Table 6. Observed and Calculated Raman and Infrared Active Frequencies of DPA, PCD, and LB (in cm^{-1})

	DPA					PCD					leucoemeraldine Base				
		this work						this work					this work		
assignment	exptl[a]	C_s	C_1	C_{2v}	calcd[a]	exptl[b]	exptl[a]	C_i	C_{2h}	calcd[a]	exptl[b]	exptl[a]	nonplanar	planar (D_{2h})	calcd[a]
(a) Raman Active Frequencies															
CC st						1617	1618	1605	1618	1617	1621	1618	1613	1624 (A_g)	1620
CC st.													1598	1613 (A_g)	
CC st (8a)[c]	1603	1606	1602	1605	1612		1604	1597	1607	1601			1593	1602 (A_g)	1603
CC st (8b)	1586	1588	1588	1591	1591	1583	1590	1590	1588	1590	1596	1597	1577	1592 (A_g)	1588
CC st, CH ipb[d] (19a)	1494	1503	1500	1501	1497	1507	1497	1507	1497	1509			1524	1507 (A_g)	
CC st, CH ipb (19b)	1456	1458	1467	1469	1462										
NH rock, CH ipb	1417	1403	1415	1424	1413	1428	1425	1424	1441	1413			1428	1378 (A_g)	1414
CH ipb (3)	1341	1328	1321	1313	1331		1341	1325	1345	1331			1319	1351 (A_g)	
CH ipb (14)	1306	1297	1301	1306	1289	1310	1309	1302	1311	1311					1315
CH ipb										1273			1272	1272 (A_g)	1295
NH rock, CH ipb		1240	1245	1241		1255	1256	1257	1260	1242			1259	1245 (A_g)	1243
CN st, CC st	1220	1205	1220	1206	1224	1212	1222	1222	1214	1220	1221	1219	1230		1217
CH ipb (9a)	1183	1181	1178	1203	1176	1193	1182	1172	1196	1176	1181	1181	1182	1188 (A_g)	1168
CH ipb (15)	1157	1151	1151	1153	1158	1156	1160	1151	1153	1155					
CH ipb (18b)	1072	1081	1086	1088	1083					1082					
CH ipb (18a)	1031	1034	1032	1040	1026	1028	1028	1035	1040	1027					
ring def (12, 1)	993	968	964	957	988	993	993	961	956	988					
ring def								958	926				931	930 (B_{2g})	
(1)						882	882	878	889	889	868	867	875	886 (A_g)	878
C1NC1′ bend	846	837	815	784	814		842	824	808	831	820	820	839	834 (A_g)	
CH opb[e]								832	809				816	801 (B_{2g})	
ring def											725	724	744	715 (A_g)	
CH opb								695	697				708	702 (B_{2g})	
CH opb						670		652	679	651	667	668	671	697 (B_{3g})	669
ring def (6a)	641	617	633	645	637								644	638 (A_g)	
ring def (6b)	611	607	611	608	595			611	598	606	603	603	612	607 (A_g)	610
ring def		555	559	561				546	550				534	534 (A_g)	
CH opb		488	490	499		517		508	506		511		481	498 (A_g)	
NH wag, CH opb		401	379	405		410		414	407		420		398	413 (B_{2g})	
NH wag, CH opb								346	335				346	341 (B_{2g})	
ring def													324	339 (B_{3g})	
(b) Infrared Active Frequencies															
CC st											1614		1612		
CC st (8a)	1596	1605	1596	1615	1599	1599	1600	1593	1606	1599					
CC st (8b)	1581	1588	1588	1591	1588	1590	1590	1592	1588	1591	1587	1596	1577	1574 (B_{2u})	
CC, CN st	1518	1503	1524	1539	1522	1535	1539	1533	1548	1534			1524	1534 (B_{3u})	
CC st						1511	1511	1509	1521	1504					1505
CC st NH rock (19a)		1490	1487	1496	1483	1495	1494	1487	1494	1493	1497	1496	1485	1502 (B_{2u})	
CC st, CH ipb (19b)		1458	1467	1469	1440	1452	1451	1454	1463	1464			1424	1458 (B_{3u})	1448
CC st, CH ipb	1417	1403	1416	1425		1396		1391	1405	1413			1368	1387 (B_{2u})	1410
CH ipb (3)	1336	1329	1332	1345	1329	1334	1335	1311	1343	1331	1283	1282	1272	1308 (B_{2u})	1280
CN st (14)	1318	1280	1316	1355	1266	1312	1311	1285	1317	1289			1259	1287 (B_{3u})	
										1252					1247
CH ipb, NH rock	1248	1245	1241	1240	1242					1242		1123		1224 (B_{3u})	1243
CN st						1225	1224	1227	1222	1220	1220	1218	1218	1207 (B_{2u})	1217
CH ipb (9a)	1172	1181	1177	1181	1177	1178	1178	1181	1197	1177	1173	1167	1199	1182 (B_{3u})	1118
CH ipb (15)	1151	1153	1152	1156	1151	1156	1155	1151	1150	1155			1182		
CH ipb						1137	1137	1151	1148	1119	1223	1107	1120	1124 (B_{2u})	1120
CH ipb (18b)	1084	1095	1086	1120	1081	1079	1077	1094	1097	1083	1107				
CH ipb (18a)	1022	1032	1035	1035	1027	1025	1026	1036	1037	1027					1016
ring def										1015	1009	1008	998	984 (B_{2u})	1014
trigonal def (12, 1)	991	966	965	958	987	993	994	992	978	987			974	973 (B_{3u})	
ring def													966	936 (A_u)	
CH opb													952	916 (A_u)	
CH opb											932		931	912 (A_u)	
def	846	859	875	878	848	875		870	868		858		880	884 (B_{2u})	
(1)						819		832	817	832	811	814	830	819 (A_u)	
CH opb						772		779	789				816	800 (A_u)	753
NH wag, CH opb	745	763	755	750		747		749	750	740	700	700	754	735 (B_{3u})	720
puckering	688	689	693	687		695		694	679						
ring def (6b)	612	618	611	608	603	614		606	592	614	621		612		
ring def		488	506	507		515		514	506		503		528	517 (A_u)	
ring def		466	490	499									482	498 (A_u)	
ring def													427	440 (B_{3u})	
NH wag		412	411	425		416		413	414				413	419 (A_u)	
NH wag		411	412	405				407	396				398	382 (A_u)	
CH opb		401	379	399				349	382				346	382 (A_u)	
CNC bending		299	295	299				346	374				312	353 (A_u)	
CNC bending								279	257				301	215 (B_{2u})	
CNC bending		186	204	138				190	213				248	212 (B_{2u})	

[a] From ref 8c. [b] From ref 8a. [c] The numbers in parentheses are benzene Wilson numbers. [d] In-plane bending. [e] Out-of-plane bending.

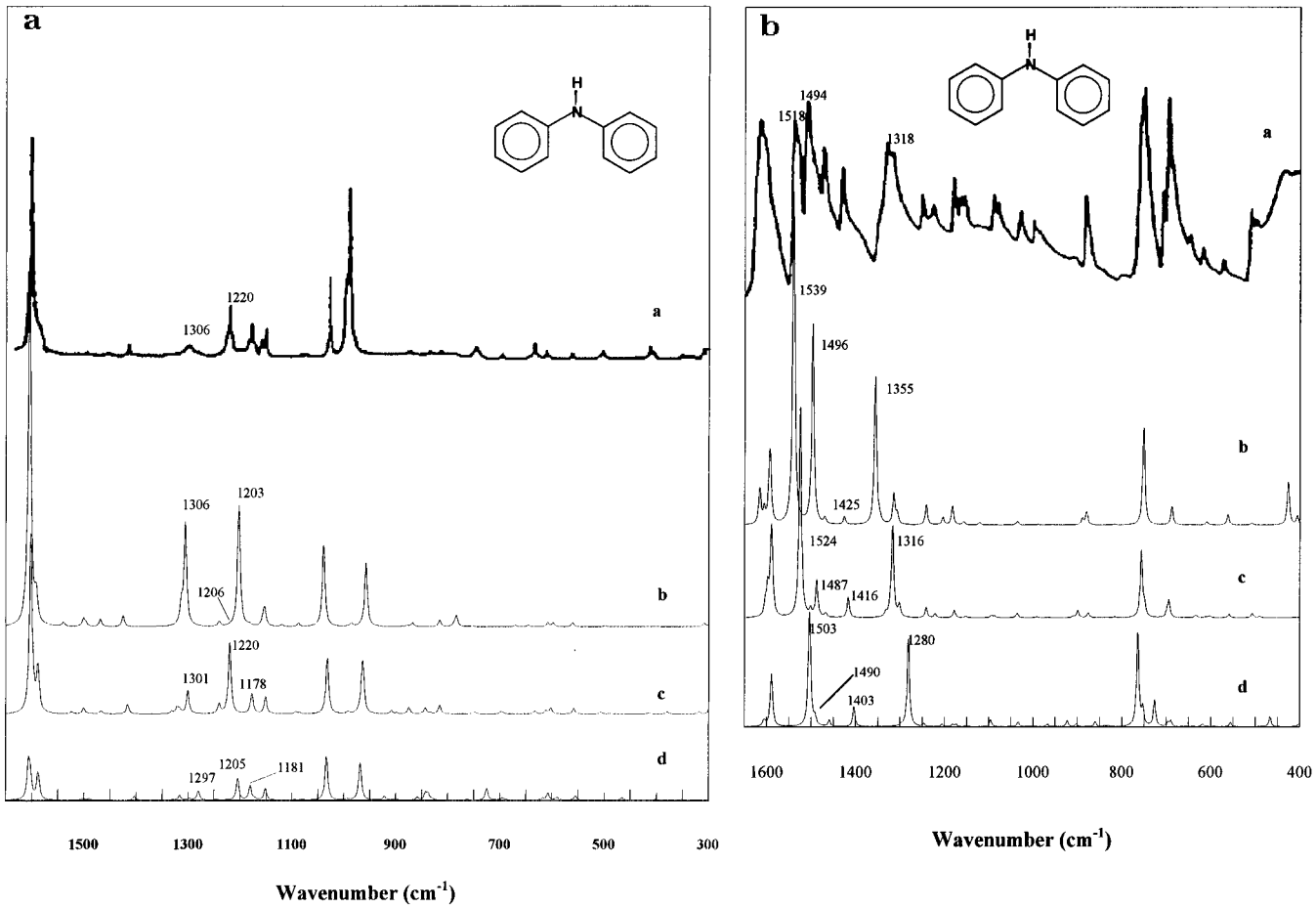

Figure 3. (a) Raman spectra of diphenylamine. Spectrum a: experimental (after ref 8b). Spectrum b: C_{2v} conformation. Spectrum c: C_1 conformation. Spectrum d: C_s conformation. (b) The IR spectra of diphenylamine. Spectrum a: experimental (after ref 8b). Spectrum b: C_{2v} conformation. Spectrum c: C_1 conformation. Spectrum d: C_s conformation.

of the phenyl ring torsional angles than the bands in the 1200−1400 cm^{-1} region. The peak at 1297 cm^{-1} (C−H in-plane bending) in C_s, however, shifts to 1301 cm^{-1} in C_1 and 1306 cm^{-1} in C_{2v}, respectively, accompanying a dramatic change of its intensity. Unfortunately, this peak is a characteristic peak of monosubstituted benzenes and cannot be used in determining the planarity of the polyaniline. The peak at 1205 cm^{-1} (C−N stretching) in C_s shifts to 1220 cm^{-1} in C_1 and 1206 cm^{-1} in C_{2v}, respectively. Note the dramatic reduction of its intensity in the C_{2v} conformation. The strongly amplified peak at 1203 cm^{-1} in C_{2v} corresponds to the 1178 cm^{-1} peak in C_1 and to the 1181 cm^{-1} peak in C_s. These last two peaks are going to be very important in determining the molecular and polymeric planarity.

Regarding the overall relative intensities of the Raman spectrum and correctly reproduced band at 1220 cm^{-1}, the C_1 conformation seems most probable. It should be noted that the ring breathing mode around 993 cm^{-1} is underestimated in our calculations, although this peak is not a characteristic peak of the LB and therefore cannot be used to obtain conformational information on LB itself.

B. PCD. The calculated vibrational spectra of PCD are presented in Figure 4 and in Table 6. In the Raman spectra, the characteristic peaks of the monosubstituted benzene ring are calculated at 956 cm^{-1} in C_{2h} and 961 cm^{-1} in C_i, 1040 cm^{-1} in C_{2h} and 1035 cm^{-1} in C_i, and 1311 cm^{-1} in C_{2h} and 1302 cm^{-1} in C_i. These do not seem to be shifted much over the torsional variation, and they also disappear in the polymer spectrum. One of the two characteristic disubstituted benzene peaks is calculated at 1618 cm^{-1} in C_{2h} and 1605 cm^{-1} in C_i, the other at 1260 cm^{-1} in C_{2h} and 1257 cm^{-1} in C_i. The vibrational modes of the amine group are overestimated in C_{2h} (1441 cm^{-1}) relative to C_i (1424 cm^{-1}). The C−H in-plane bending (experiment at 1028 cm^{-1}) mode is slightly overestimated in both cases.

There are two conformation-dependent peaks in the Raman spectrum of PCD. The peak at 1172 cm^{-1} in C_i is blue-shifted to 1196 cm^{-1} in C_{2h} and strongly gains intensity. The peak at 1222 cm^{-1} in C_i is red-shifted to 1214 cm^{-1} and loses intensity. We have seen the same behavior from the simulation of the DPA Raman spectra.

Quillard et al.[8c] pointed out that their spectrum was in good agreement with previously reported data by Furukawa *et al.*,[8a] except for these particular two bands. Furukawa *et al.* reported the two frequencies 1193 and 1212 cm^{-1}, while Quillard *et al.* observed them at 1182 and 1222 cm^{-1}. Quillard *et al.* suggested that these differences provide evidence for weak intermolecular coupling of crystalline PCD with respect to an amorphous sample. The results of our calculations offer a refinement of this picture. Accordingly, the peaks at 1196 and 1214 cm^{-1} in C_{2h} can be assigned to the peaks at 1193 and 1212 cm^{-1} reported by Furukawa *et al.*,[8a] respectively. These differences of intensity and peak position arise from differences in the molecular conformation, specifically, torsional angles. In crystalline PCD, the overall ring-torsional angles are reduced so as to allow more compact packing. Therefore, these peak positions together with the relative intensities

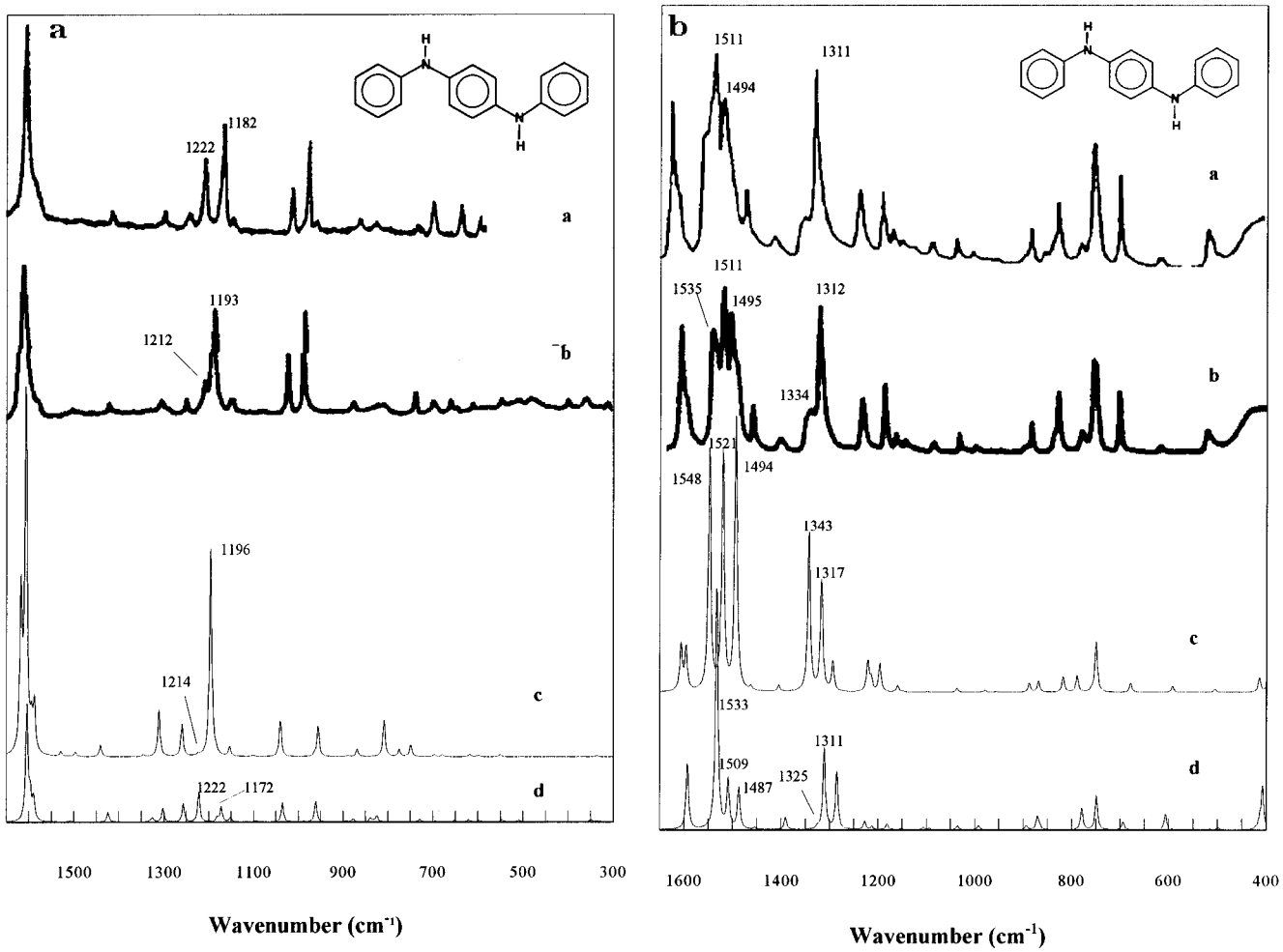

Figure 4. (a) Raman spectra of PCD. Spectrum a: experimental (after ref 8c). Spectrum b: experimental (after ref 8a). Spectrum c: C_{2h} conformation. Spectrum d: C_i conformation. (b) IR spectra of PCD. Spectrum a: experimental (after ref 8c). Spectrum b: experimental (after ref 8a). Spectrum c: C_{2h} conformation. Spectrum d: C_i conformation.

might be good indicators of molecular planarity. According to this evidence, it is likely that the conformations in the two samples are different and that Furukawa's sample might be more planar than those of Quillard *et al.*

C. ACT and Polymeric LB. Planar PCD (C_{2h}) was used as a model oligomer for the vibrational analysis of the planar conformation of the LB polymer using eq 1. Since the planar model has a 180° screw axis along the polymer backbone, vibrational modes both at the center and at the edge of the Brillouin zone are active. (Quillard et al.[8c] have reported only the $k = 0$ modes.) We used another oligomer, the aniline end-capped trimer (ACT), as a model compound for the repeat unit of the nonplanar conformation of the LB polymer. If the polymer is not planar, the two phenyl ring torsional angles have to alternate in order to retain translational symmetry along the polymer chain. Otherwise, a helical system will be formed. In this alternating torsional angle case, the unit cell of the polymer has two nonequivalent phenyl rings (see Figure 1e), and due to the absence of the screw axis of symmetry only the $k = 0$ modes are active. Note, that since the magnitudes of the two phenyl torsional angles are different, the unit cell is doubled relative to the planar model.

Using these two model compounds, the predicted vibrational spectra of the polymer in two conformations are presented in Figure 5 and Table 6. There is a satisfactory overall agreement between the experimental spectra and the planar predicted spectra. Note that no experimental information from any spectra other than the 12 aniline scaling factors went into this calculation. We have found that the band around 1620 cm^{-1} is composed of three peaks. The experimental peaks at 1219 (1221) and 1181 cm^{-1} are calculated at 1230 and 1182 cm^{-1} in the nonplanar model and at 1224 and 1188 cm^{-1} in the planar model, respectively. However, the symmetry of the calculated peak at 1224 cm^{-1} in the planar model is B_{3u} within the D_{2h} point group. Consequently, this band is not Raman active in the harmonic approximation (see Table 6). Quillard *et al.*,[8c] however, have calculated the corresponding peak at 1217 cm^{-1} and assigned it to a Raman active mode using their empirical force field calculation while calculating the nearby IR active experimental peak at 1219 (1221) cm^{-1} also at 1217 cm^{-1}.

Regarding the symmetry of the peak at 1219 (1221) cm^{-1}, the necessary condition for Raman activity of this peak is the absence of inversion symmetry in the polymer. To satisfy this condition, the magnitude of the two adjacent torsional angles around bridging nitrogen should be different. The observed Raman spectra exhibit a weak peak at 1219 (1221) cm^{-1} indicating slight nonplanarity. As we have seen, the change of the ratio between the two peaks at 1220 cm^{-1} and at 1180 cm^{-1} indicates changes of conformation in the simulated Raman spectra of the oligomers. Therefore, the intensity ratio of these two bands can be used to quantita-

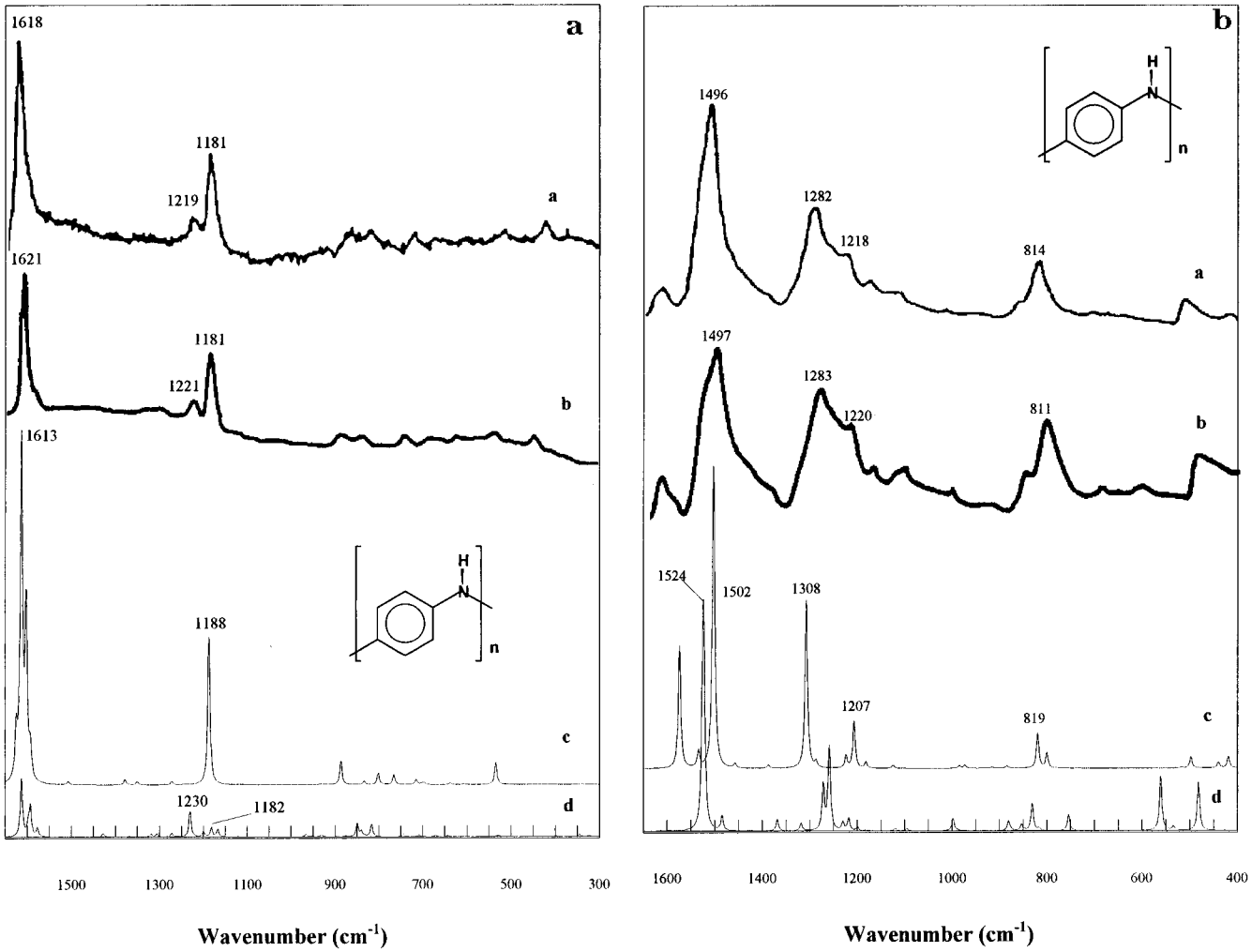

Figure 5. (a) Raman spectra of leucoemeraldine base. Spectrum a: experimental (after ref 8c). Spectrum b: experimental (after ref 8a). Spectrum c: planar conformation. Spectrum d: nonplanar conformation. (b) IR spectra of leucoemeraldine base. Spectrum a: experimental (after ref 8c). Spectrum b: experimental (after ref 8a). Spectrum c: planar conformation. Spectrum d: nonplanar conformation.

tively characterize the degree of planarity in the polymer.

6. Infrared Spectra of Leucoemeraldine Base and Its Oligomers

A. DPA. The calculated IR spectra of DPA (see Figure 3b and Table 6b) exhibit more noticeable variations than the Raman spectra as a function of conformational changes. The peak at 1503 cm^{-1} in C_s (C−C stretching, C−H in-plane bending, and N−H rocking) is blue-shifted to 1524 cm^{-1} in C_1 and to 1539 cm^{-1} in C_{2v}, respectively. The peak at 1496 cm^{-1} in C_{2v} (C−C stretching and N−H rocking) corresponds to the peaks at 1487 cm^{-1} in C_1 and 1490 cm^{-1} in C_s. The dipole moment derivative and consequently the peak intensity of the N−H rocking mode are greatly increased in the C_{2v} conformation as compared to the other conformations. Near planarity around the nitrogen seems to increase the magnitude of the dipole moment derivative with respect to the N−H rocking mode.

The peak at 1403 cm^{-1} (C−H in-plane bending and C−C stretching) in C_s is blue-shifted to 1416 cm^{-1} in C_1 and to 1425 cm^{-1} in C_{2v}. The 1280 cm^{-1} mode in C_s (mostly C−N stretching) is blue-shifted to 1316 cm^{-1} in C_1 and 1355 cm^{-1} in C_{2v}, showing large frequency dispersion with respect to conformation. As can be seen from Figure 3b, the out-of-plane modes around 700−800 cm^{-1} are red-shifted as the molecular planarity is increased. Overall, the spectrum based on the C_1 structure agrees best with the experiment. The same conclusion was drawn from the Raman spectra for DPA also.

B. PCD. In the IR spectra of PCD (see Figure 4b), the peaks at 1533 and 1509 cm^{-1} in C_i shift to 1548 cm^{-1} and 1521 cm^{-1}, respectively. The intensity at 1494 cm^{-1} in C_{2h} (1487 cm^{-1} in C_i), which is attributed to N−H rocking, is greatly increased in the planar conformation. The peaks at 1311 cm^{-1} (C−N stretching) and 1285 cm^{-1} (C−H in-plane bending) in C_i are blue-shifted to 1343 and 1317 cm^{-1} in C_{2h}, respectively.

In contrast to DPA, this simulation of the IR vibrational spectrum, together with the Raman discussion in section 5, points to a clear preference of the C_{2h} conformation. The actual conformation of PCD might be closer to the planar form or a mixture of more than one conformation. Even though the C_i conformation is energetically more stable, intermolecular forces seem to be the governing factor in determining the molecular conformation of PCD.

C. Leucoemeraldine Polymer. The observed IR spectrum of LB exhibits several broad bands (see Figure 5b). The major bands are at 1596 cm^{-1} (C−C stretching), 1497 cm^{-1} (ring stretching), 1283 cm^{-1} (C−H in-plane bending and C−N stretching), and 1220 and 811

Table 7. Diagonal Force Constants (in mdyn/Å)[a]

	DPA			PCD	
	C_s	C_1	C_{2v}	C_1	C_{2h}
C1−N	5.83	6.30	6.43	6.18	6.49
C1′−N	5.83	6.24	6.43	6.16	6.32
C1−C2	6.71	6.64	6.60	6.67	6.59
C1′−C2′	6.71	6.58	6.60	6.75	6.66
C2−C3	6.90	6.84	6.76	6.83	6.76
C2′−C3′	6.90	6.95	6.76	6.91	6.98
C3−C4	6.87	6.93	7.09	6.97	7.09
C3′−C4′	6.87	6.82	7.09	6.72	6.75
C4−C5	6.92	6.83	6.79	6.82	6.78
C4′−C5′	6.92	6.93	6.79	6.75	6.66
C5−C6	6.87	6.99	7.15	7.04	7.17
C5′−C6′	6.87	6.87	7.15	6.91	6.98
C6−C1	6.70	6.61	6.45	6.58	6.42
C6′−C1′	6.70	6.71	6.45	6.72	6.75
N−H	6.53	6.71	6.77	6.67	6.78
NH rocking	0.82	0.91	1.42	0.91	1.39

[a] Atom numbering is defined in Figure 1.

cm^{-1} (C−H out-of-plane bending). The peak at 1596 cm^{-1} (C−C stretching) is calculated at 1574 cm^{-1} in the planar model. The broad band around 1497 cm^{-1} was assigned to C−C stretching and C−H in-plane bending.[8a] We have seen the strongly increased intensities of the N−H rocking mode in DPA (1496 cm^{-1} in C_{2v}) and PCD (1494 cm^{-1} in C_{2h}) cases; this broad band also has a contribution from N−H rocking. The bands at 1283 and 1218 cm^{-1} were assigned to mixed modes of C−H bending and C−N stretching.[11] Those peaks were calculated at 1308 and 1207 cm^{-1} in our planar model, and at 1272 and 1218 cm^{-1} in the nonplanar model, respectively. However, Quillard *et al.*,[8c] have reassigned these bands to C−H bending and C−N stretching modes, respectively. According to our calculation, however, the original assignments by Furukawa were correct.

As compared with the vibrational assignments of Quillard *et al.* for the polymer,[8c] we have found a few disagreements. However, we agree with their major conclusion: both IR and Raman spectra indicate that LB is close to planar.

Even though energetically the nonplanar conformation is more stable by about 3−4 kcal/mol per phenyl ring, our polymeric normal mode analysis clearly shows the preference of a more planar model in interpreting the vibrational spectra of the samples. In terms of force constants, our diagonal oligomer force constants are somewhat larger than those of Quillard *et al.* (see Table 7). As expected, the force constants of C−N stretching and N−H rocking are more sensitive to molecular conformation than the C−C stretching ones.

7. Electronic Structure of Leucoemeraldine Base

As we mentioned earlier, Brédas *et al.*[1d] have calculated the ring-torsional angle dependence of the band structures of polyaniline. They have used the nonempirical non-SCF valence effective Hamiltonian (VEH)[19] method based on the nonplanar AM1 optimized geometries of a four-ring oligomer of LB and found that in this model there is no dimerization of the ring-torsion angles in the ground state of LB. They have shown that the band gap varies only slightly, from 3.77 to 4.05 eV, as a function of ϕ assuming that $\phi - \phi'$ is kept constant (see Table 8). They have not considered a planar model, which is certainly an energetically higher conformation, as discussed in the previous sections. On the other hand, on the basis of the vibrational spectroscopic evidence supporting a nearly planar LB structure, we have extended band structure studies to include this conformation also (PCD-based structure) in addition to the nonplanar one (ACT-based structure). These results are also given in Table 8. As indicated by the data in Table 9 and discussed earlier in ref 20, this methodology gives a reasonable description of the band gap of the pernigraniline base form as well. Therefore, the calculated band gap should provide further evidence concerning the conformation of the LB form also.

Table 8. Experimental and Theoretical Band Gap of Leucoemeraldine Base (in eV)

	ϕ[a]	ϕ' [a]	E_g
VEH/AM1[b]	30	30	3.77
	0	60	4.05
MEHT/HF/6-31G* [c]	0	0	4.29
	15.5	87.5	5.08
exptl[d]			3.6−3.8

[a] These angles are defined in Figure 1. [b] Taken from ref 1d. [c] This work. [d] Taken from ref 21.

Table 9. Experimental and Theoretical Band Gap of Pernigraniline Base (in eV)

	ϕ[a]	ϕ' [a]	E_g
VEH/AM1[b]	30	30	0
	0	60	0.66
MEHT/HF/6-31G* [c]	0	0	1.14
	4.1	61.4	1.92
exptl[d]			1.65

[a] These angles are similarly defined as in Figure 1e. [b] Taken from ref 1d. [c] This work. [d] Taken from ref 21.

The calculated band gaps of the planar and nonplanar models of LB described in this paper are 4.29 and 5.08 eV. These results show a relatively strong dependence on the torsional dimerization. This is a consequence of the significant overlap between the N and phenyl π orbitals in the planar or nearly planar conformations that is largely reduced in the nonplanar one. This picture agrees qualitatively with the MO diagrams for the highest occupied and lowest unoccupied crystal orbitals given in another paper by Brédas *et al.*[1f] The calculated band gap of our planar model is about 0.5 eV higher than the experimental value.[21] However, the band-gap difference between our two conformations (0.79 eV) is large enough to lend further qualitative support to our planar or nearly planar model for LB.

8. Conclusions

We have performed *ab initio* geometry optimizations and normal mode analyses on a series of oligomers of an important polyaniline, LB. We have found several conformation-dependent vibrational bands. Most of these bands are attributed to C−N, C−H in-plane bending, and N−H rocking modes.

Some of these bands also show a strong relationship between intensity and π conjugation. In DPA, some modes assigned to C−N stretching, N−H rocking, and C−H in-plane bending are strongly dependent on molecular planarity, indicating coupling between in-plane modes and molecular conformations. Both IR and Raman intensities increase as we move from C_1 to C_s to C_{2v} symmetry. This implies that there is a close relationship between p−π conjugation and the dipole moment derivatives and the polarizability derivatives.

With the help of *ab initio* normal mode analysis and SQMOFF,[9] we have performed a complete normal mode assignment of LB. Combing the geometric data and vibrational spectra, we have found that the best de-

scription of the vibrational spectra is achieved if we assume that the conformation of these systems depends on their length. In contrast to the favorable C_1 conformation in DPA, the oligomeric systems assume more planar conformations as the size of the oligomer is increased. This result tells us that the intermolecular packing forces may be significant enough to cause conformational changes and make the planar or nearly planar conformation more stable in the polymeric system. These results are further supported by our energy band calculations on the electronic structure of LB. We concluded that a nearly planar form is the most probable structure for LB. However, the observed Raman spectra still exhibit a characteristic band due to nonplanarity (around 1220 cm^{-1}). The intensity ratio between the two Raman bands at 1220 and 1180 cm^{-1} may be utilized in determining the degree of polymeric planarity in a given sample.

We think that our calculations presented here can provide a starting point to understand the structural and conformational evolution of other members of the polyaniline family upon doping and/or chemical treatment. We are planning to extend our calculations to other members of the polyaniline family of materials in order to gain insight into their structures through the interpretation of their vibrational spectra.

Acknowledgment. We thank the National Science Foundation, Pittsburgh Supercomputing Center (PSC, DMR-920006P), and the National Center for Supercomputing Applications (NCSA, DMR-950029N) for the use of supercomputing facilities.

References and Notes

(1) (a) MacDiarmid, A. G.; Chiang, J. C.; Richter, A. F.; Epstein, A. J. *Synth. Met.* **1987**, *18*, 285. (b) Chiang, J. C.; MacDiarmid, A. G. *Synth. Met.* **1986**, *13*, 193. (c) Shacklette, L. W.; Wolf, J. F.; Gould, S.; Baughman, R. H. *J. Chem. Phys.* **1988**, *88* (6), 3955. (d) Brédas, J. L.; Quattrocchi, C.; Libert, J.; MacDiarmid, A. G.; Ginder, J. M.; Epstein, A. J. *Phys. Rev. B* **1991**, *44* (12), 6002. (e) Masters, J. G.; Ginder, J. M.; MacDiarmid, A. G.; Epstein, A. J. *J. Chem. Phys.* **1992**, *96* (6), 4768. (f) Libert, J.; Brédas, J. L.; Epstein, A. J. *Phys. Rev. B* **1995**, *51* (9), 5711.

(2) MacDiarmid, A. G.; Epstein, A. J. *Faraday Discuss. Chem. Soc.* **1989**, *88*, 317.

(3) Peierls, R. *Quantum Theory of Solids*; Oxford: 1955.

(4) Ginder, J. M.; Epstein, A. J.; MacDiarmid, A. G. *Solid State Commun.* **1989**, *72*, 987.

(5) Ginder, J. M.; Epstein, A. J. *Phys. Rev. B* **1990**, *41*, 10674.

(6) Starikova, Z. A. *J. Struct. Chem.* **1989**, *30*, 301.

(7) Ito, A.; Ota, K.; Yoshizawa, K.; Tanaka, K.; Yamabe, T. *Chem. Phys. Lett.* **1994**, *223*, 27.

(8) (a) Furukawa, Y.; Ueda, F.; Hyodo, Y.; Harada, I.; Nakajima, T.; Kawagoe, T. *Macromolecules* **1988**, *21*, 1297. (b) Quillard, S.; Louarn, G.; Buisson, J. P.; Lefrant, S.; Masters, J.; MacDiarmid, A. G. *Synth. Met.* **1992**, *49*, 525. (c) Quillard, S.; Louarn, G.; Lefrant, S.; MacDiarmid, A. G. *Phys. Rev. B* **1994**, *50* (17), 12496. (d) Kostic, R.; Rakostic, D.; Davidova, I. E.; Grobov, L. A. *Phys. Rev. B* **1992**, *45*, 728.

(9) Cui, C. X.; Kertesz, M. *J. Chem. Phys.* **1990**, *93*, 5257.

(10) (a) Cuff, L.; Kertesz, M. *Macromolecules* **1994**, *27*, 762. (b) Cuff, L.; Kertesz, M.; Geisselbrecht, J.; Kurti, J.; Kuzmany, H. *Synth. Met.* **1993**, *55*, 564. (c) Cuff, L.; Kertesz, M. *J. Phys. Chem.* **1994**, *98*, 12223. (d) Cuff, L.; Cui, C. X.; Kertesz, M. *J. Am. Chem. Soc.* **1994**, *116*, 9269. (e) Cuff, L. Kertesz, M. *Polym. Prepr.* **1994**, *35* (2), 792.

(11) (a) Born, M.; Von Karman, T. *Phys. Z.* **1912**, *13*, 287. (b) Born, M.; Huang, K. *Dynamical Theory of Crystal Lattices*; Clarendon Press: Oxford, 1954.

(12) Wilson, E.; Decius, J.; Cross, P. *Molecular Vibrations*; McGraw-Hill: 1955.

(13) Frisch, M. J.; Trucks, G. W.; Schlegel, H. B.; Gill, P. M. W.; Johnson, B. G.; Robb, M. A.; Cheeseman, J. R.; Keith, T.; Petersson, G. A.; Montgomery, J. A.; Raghavachari, K.; Al-Laham, M. A.; Zakrzewski, V. G.; Ortiz, J. V.; Foresman, J. B.; Cioslowski, J.; Stefanov, B. B.; Nanayakkara, A.; Challacombe, M.; Peng, C. Y.; Ayala, P. Y.; Chen, W.; Wong, M. W.; Andres, J. L.; Replogle, E. S.; Gomperts, R.; Martin, R. L.; Fox, D. J.; Binkley, J. S.; Defrees, D. J.; Baker, J.; Stewart, J. P.; Head-Gordon, M.; Gonzalez, C.: Pople, J. A. Gaussian, Inc.: Pittsburgh, PA, 1995.

(14) Pople, J. A.; Schlegel, H. B.; Krishnan, R.; Defrees, D. J.; Binkley, J. S.; Frisch, M. J.; White, R. A.; Hout, R. F.; Hehre, W. J. *Int. J. Quantum Chem., Quantum Chem. Symp.* **1981**, No. 15, 267.

(15) Pulay, P.; Fogarasi, G.; Boggs, J. E.; Vargha, A. *J. Am. Chem. Soc.* **1983**, *105*, 7037.

(16) Pulay, P; Fogarasi, G.; Pang, F.; Boggs, J. E. *J. Am. Chem. Soc.* **1979**, *101*, 2550.

(17) (a) Evans, J. C. *Spectrochim. Acta* **1960**, *16*, 428.(b) Rauhut, G.; Pulay, P. *J. Phys. Chem.* **1995**, *99*, 3093.

(18) Hong, S. Y.; Marynick, D. *J. Chem. Phys.* **1992**, *96*, 5497.

(19) Brédas, J. L.; Chance, R. R.; Silbey, R.; Nicolas, G.; Durand, Ph. *J. Chem. Phys.* **1981**, *75*, 255.

(20) Kertesz, M.; Choi, C. H.; Hong, S. Y. *Syn. Met.*, in press.

(21) McCall, R. P.; Ginder, J. M.; Leng, J. M.; Yee, H. J.; Manohar, S. K.; Masters, J. G.; Asturias, G. E.; MacDiarmid, A. G.; Epstein, A. J. *Phys. Rev. B* **1990**, *41*, 5202.

(22) Niu, Z.; Dunn, K. M.; Boggs, J. E. *Mol. Phys.* **1985**, *55* (2), 421.

(23) Brassy, C.; Mornon, J. P. *C. R. Seances Acad. Sci. (Paris)* **1972**, *C274*, 1728.

MA961120N